Serb. Astron. J. № 173 (2006), 35 - 47 **UDC 524.7–42–73**
DOI:10.2298/SAJ0673035S Original scientific paper

GLOBULAR CLUSTERS AND PLANETARY NEBULAE KINEMATICS AND X–RAY EMISSION IN THE EARLY–TYPE GALAXY NGC 5128

S. Samurović

Astronomical Observatory, Volgina 7, 11160 Belgrade 74, Serbia

(Received: June 26, 2006; Accepted: September 6, 2006)

SUMMARY: The estimates of the mass of the galaxy NGC 5128 based on the different mass tracers, globular clusters (GCs) and planetary nebulae (PNe), are presented. These estimates are compared with the estimate based on the X–ray methodology and it is found that the results for the mass (and mass-to-light ratio) for all three approaches are in very good agreement interior to 25 arcmin; beyond 25 arcmin the X–rays predict the mass which is too high with respect to the one found using GCs and PNe. Some possible explanations for this discrepancy were discussed. The Jeans equation is also solved and its predictions for the velocity dispersion are then compared with the observed values, which extend to $\sim$ 8 effective radii in the case of the GCs and $\sim$ 15 effective radii in the case of the PNe. It is found that interior to $\sim$ 25 arcmin ($\sim$ 5 effective radii) dark matter does not dominate because the total mass-to-light ratio in the B–band in solar units is less than 10. Based on the GCs and PNe beyond $\sim$ 25 arcmin the total mass-to-light ratio increases to $\sim$ 14 (at $\sim$ 80 arcmin) which indicates the existence of dark matter in the outer regions of NGC 5128.

Key words. Galaxies: kinematics and dynamics – Galaxies: elliptical and lenticular, cD – Galaxies: structure – dark matter – Galaxies: individual (NGC5128)

1. INTRODUCTION

The problem of dark matter remains to be one of the most important unresolved problems in cosmology and astronomy. The situation regarding dark matter in spiral galaxies seems to be rather clear because in these galaxies there exists a cool gas which provides a powerful tool for obtaining rotation curves, that are, for most spirals, nearly flat thus indicating the presence of dark mass in their outer parts – dark haloes (see e.g. Binney and Tremaine 1987). On the other hand, early–type galaxies (ellipticals and lenticulars) contain little or no cool gas so one cannot use 21-cm observations to trace kinematics of neutral hydrogen out to large radii.

The external regions of elliptical galaxies are of special importance because these are regions where dark matter might be expected to dominate luminous matter. We briefly describe below the possible methodologies for tracing of dark matter in early type galaxies. Studies which use integrated stellar light are limited to 3 to 4 effective radii (one effective radius, R_e, is the radius of the isophote containing half the total luminosity) because of the low surface brightness beyond these regions. If one wishes to study the mass distribution beyond $\sim$ 3 effective radii one can use the X–ray methodology which analyzes hot gas at temperatures $\sim 10^7$ K or planetary nebulae and globular clusters.

Here we briefly quote an estimate of the typical mass-to-light ratio in elliptical galaxies by van der Marel (1991) who found in his sample of 37 bright ellipticals that the average mass-to-light ratio in the B–band in solar units (it is assumed

that solar units are used throughout this paper) is: $M/L_B = (5.95 \pm 0.25)h_{50}$ thus $M/L_B = 8.33 \pm 0.35$ for $h_0 = 0.70$ (the value of the Hubble constant used in this paper). He also found that the mass-to-light ratio is correlated with the total luminosity: $M/L_B = 3.84h_{50}(L_B/L_{*,B})^{0.35}$, where $L_{*,B} \equiv 3.3 \times 10^{10}h_{50}^{-2}L_{\odot}$.

These are the possible approaches to check whether early–type galaxies do have dark matter haloes:

(i) *Stellar kinematics* – the great obstacle is the fact that their outer parts are very faint, and it is therefore usually difficult to obtain spectra to constrain kinematics at large radii. This method based on *the integrated stellar light* provides data out to ~ 3 to 4 effective radii (see e.g. Carollo et al. 1995, Statler, Smecker–Hane and Cecil 1996, Kronawitter et al. 2000, Samurović and Danziger 2005, hereafter SD05). Using this methodology, it seems that dark matter (at least in some galaxies) does not dominate interior to $\sim 3R_e$. Note that recently, on the theoretical grounds, Mamon and Łokas (2005) found that the stellar component should dominate the dark matter component out to at least 1 R_e.

(ii) *X–rays*, a consequence of the existence of the hot gas at the temperature $T \sim 10^7$ K, found in a large number of massive early–type galaxies (interestingly, not in all, see the case of IC 3370 from SD05) is an extremely useful tool for the study of the mass because the methodology is well known (some important details for the sake of clarity will be repeated below). The present observational situation is interesting: for example, Sivakoff et al. (2004) used the X–ray observations by CHANDRA and assuming hydrostatic equilibrium found that for the X–ray bright galaxy NGC 1600 within $\sim 4R_e$ dark matter does not dominate. But two very recent studies based on the CHANDRA data by Humphrey et al. (2006) and Fukazawa et al. (2006) used the same methodology (on different samples) on X–ray data to demonstrate the existence of dark matter beyond $\sim 1R_e$.

(iii) *Planetary nebulae (PNe)* are a very promising tool for dark matter research because they are detectable even in moderately distant galaxies through their strong emission lines. For example, Hui et al. (1995) found that the mass-to-light ratio in the central region of a giant elliptical galaxy NGC 5128 is ~ 3.9 and that out to ~ 5 R_e it increases to ~ 10 (in the B-band), thus indicating the existence of the dark halo. Since this galaxy is the subject of the present work more details will be given below. Here we note briefly the Romanowsky et al. (2003) observations of PNe in three galaxies (NGC 821, NGC 3379 and NGC 4494) which claim little or no dark matter out to ~ 3.5 R_e (if one takes into account a correct value of the effective radius for NGC 3379, see SD05 for details). Very recently, Sluis and Willams (2006) used the Rutgers Fabry–Pérot in order to search for planetary nebulae in NGC 3379 and three other galaxies in order to use the PNe as kinematic tracers of the galaxy potential. They detected 54 PNe in NGC 3379 and found that within $\sim 5R_e$ the total mass-to-light ratio in the B–band of this galaxy is ~ 5 implying very low amount of dark matter in the given region (~ 130 arcsec).

(iv) *Globular clusters (GCs)* can also be used as tracers of dark matter in the early-type galaxies: Mould et al. (1990) found for two giant elliptical galaxies M49 and M87 from the Virgo cluster that the velocity dispersion profiles of the cluster systems were flat, thus suggesting the existence of an isothermal halo of dark matter in these elliptical galaxies. Grillmair et al. (1994) studied the radial velocities of 47 globular clusters in NGC 1399 in the Fornax cluster od galaxies. Under the assumption that the clusters were on purely circular orbits, they gave a lower limit on a globally constant mass-to-light (M/L_B) ratio of 79 ± 20 in the B-band. Their result, suggesting that M/L is several times larger than values of mass-to-light ratio determined from the stellar component closer to the core, implies that M/L_B must increase substantially with radius. This result was confirmed in a recent paper by Samurović and Danziger (2006) who used the recent observations of NGC 1399 by Dirsch et al. (2003), Richtler et al. (2004) and Dirsch et al. (2004) to find that in spite of the observations that show that the velocity dispersion decreases between 4 and 10 R_e there is evidence that dark matter exists beyond $\sim 3R_e$ (but does not dominate interior to this distance). Another example is that of M49 (= NGC4472) studied by Côté et al. (2003) who showed that the globular clusters radial velocities and density profiles provide "unmistakable evidence" for a massive dark halo. Very recently, Pierce et al. (2006) have obtained Gemini/GMOS spectra for 22 GCs associated with NGC 3379 and found that, in contrast to the results of Romanowsky et al. (2003), their results suggest a constant value of the velocity dispersion (out to ~ 200 arcsec) which imply a normal–sized dark matter halo. They do note, however, that due to possible anisotropies (see below) they could not rigourously determine the dark halo mass.

(v) *Weak gravitational* lensing enables determination of the dependence of the velocity dispersion on the luminosity of the lensing galaxies and is suitable for studies of the dark matter in outer part of galaxies. It was found that a Navarro-Frenk-White (NFW) profile provides a good fit to the data (Kleinheinrich et al. 2003). *Strong gravitational lenses* can also be used for probing of the galaxy haloes, but only in the inner regions of galaxies (few tens of kiloparsecs) (see e.g. Prada

et al. 2003). The Lenses Structure and Dynamics (LSD) Survey gathers kinematic data for distant (up to $z \sim 1$) early-type galaxies that are gravitational lenses (review in Treu et al. 2003). The results of this survey suggest that extended dark matter haloes are detected in the early-type galaxies and that the dark matter contributes 50-75% to the total mass within the Einstein radius (cases of the lens galaxies MG2016+112 in Treu and Koopmans (2002) and 0047-281 in Koopmans and Treu (2003).

A serious problem with the determination of the mass in the early–type galaxies is related to the fact that one does not *a priori* know anything about the orbits of stars in ellipticals which leads to a well known mass–anisotropy degeneracy (see Tonry 1983: see also Binney and Merrifield 1998, Chap 11.2).

From what was said so far it seems obvious that current investigations lead to the conclusion that there is less unambiguous evidence for the dark matter in ellipticals than in the case of spirals. The currently popular theoretical cosmological models (such as cold dark matter, CDM, models, but see the very recent criticism of the CDM models in Gibson 2006) predict huge amounts of dark matter in these galaxies, but as it was shown above some recent observations fail to confirm this for particular galaxies (see e.g. Romanowsky et al. (2003), Peng et al. (2004b), SD05) at least in regions interior to 3–5 effective radii. Dekel et al. (2005) used numerical simulations to show that dark matter in early–type galaxies in fact exists, but that a careful modelling is needed because radial orbits may dominate. Also, some recent works claim to detect the presence of dark matter in ellipticals interior to smaller distances from the galactic center (see e.g. Thomas et al. 2005, Teodorescu et al. 2005, Cappellari et al. 2006, De Rijcke et al. 2006).

The example of the galaxy NGC 5128 is an interesting one because different observations based on different techniques are available making thus possible a thorough comparison out to large distance from the center (out to $\sim 15R_e$).

The plan of this paper is as follows: In Section 2 we present the basic observational data related to NGC 5128 concerning photometry, GCs, PNe and X–rays and the results concerning its kinematics. In Section 3 we present the X–ray modelling of NGC 5128; using the results thus obtained the Jeans modelling is performed. In Section 4 the mass estimates of NGC 5128 based on a new "tracer mass estimator" are given and compared with the previously established X–ray estimates. Finally, in Section 5 the conclusions are drawn.

2. OBSERVATIONAL DATA AND KINEMATICS OF NGC 5128

2.1. NGC 5128 (Cen A)

NGC 5128 (also known as the radio source Centaurus A) is the nearest large elliptical galaxy. The value of the distance used in this paper, $D = 3.84 \pm 0.35$ Mpc is taken from the paper by Rejkuba (2004) and is in agreement with other estimates found in the literature (such as Hui et al. 1993). At this distance $1' \approx 1$ kpc. NGC 5128 is the only early–type member of the Centaurus group. In this paper the adopted center of the galaxy is $(13^{\rm h}25^{\rm m}27\overset{\rm s}{.}72, -43°01'05\overset{''}{.}8$,J2000). The effective radius is $R_e = 5.3$ kpc and the systemic velocity is $v_{\rm syst} = 541$ km s^{-1}. The B–band luminosity of the stellar component NGC 5128 is $L_B = 3.98 \times 10^{10} L_\odot$. The complete review of this galaxy can be found in the paper by Israel (1998). Because of its proximity and interesting features (observational evidence of one or more major merging events) NGC 5128 is an excellent target for a detailed study: a large number of papers with a wealth of observational data is available which makes it possible to investigate its properties by comparing different observations (in the present paper, GCs, PNe and X–rays).

2.2. Globular clusters of NGC 5128

The sample which was used in this paper was built using two different samples: (i) the first one is taken from the paper by Peng et al (2004a) who conducted an optical and spectroscopic survey for GCs across $\sim 1°$ of sky around NGC 5128 and includes 215 clusters: their whole sample was taken and (ii) the second one is taken from the paper by Woodley, Harris and Harris (2005) who measured radial velocities for 74 GCs: in this case 31 GCs not present in the previous sample were taken. In total we use 246 clusters which extend out to 42.44 kpc ($= 8R_e$). The kinematics of NGC 5128 based on the GCs is given in Table 1 and also in Fig. 1: from the top to the bottom we plot as function of radius, radial velocity, velocity dispersion, s_3 and s_4 parameters (for the description of these quantities see Section 2.5).

2.3. Planetary nebulae of NGC 5128

The sample of PNe used in this paper comes from the paper by Peng et al. (2004b) and contains 780 PNe. The kinematics of NGC 5128 based on the PNe is given in Table 2 and also in Fig. 2 (the meaning of symbols is the same as in the case of GCs). Note that error bars are not plotted in the case of radial velocities: as given in Peng et al. (2004b) they are taken to be 20 km s^{-1} in the calculations below. The data for the PNe extend out to 78 arcmin ($= 14.7R_e$).

2.4. X–ray data for NGC 5128

The analysis of NGC 5128 based on the results from two Chandra/ACIS-I observations and one XMM-Newton observation of X-ray emission from the interstellar medium (ISM) is given in Kraft et al. (2003). It was found that the ISM has an average radial surface brightness profile that is well described by a β-model profile with index $\beta = 0.40 \pm 0.04$ and

a temperature of $k_B T_{\rm ISM} = 0.29$ keV beyond 2 kpc from the galactic nucleus. These data will be used below when we calculate the total mass and the total mass-to-light ratio of NGC 5128.

2.5. Mathematical background and kinematics of NGC 5128

The determination of the kinematical parameters can be done using different techniques. It was shown in Samurović and Danziger (2006) that the results based on the maximum likelihood method and those using standard statistical definitions do not differ,

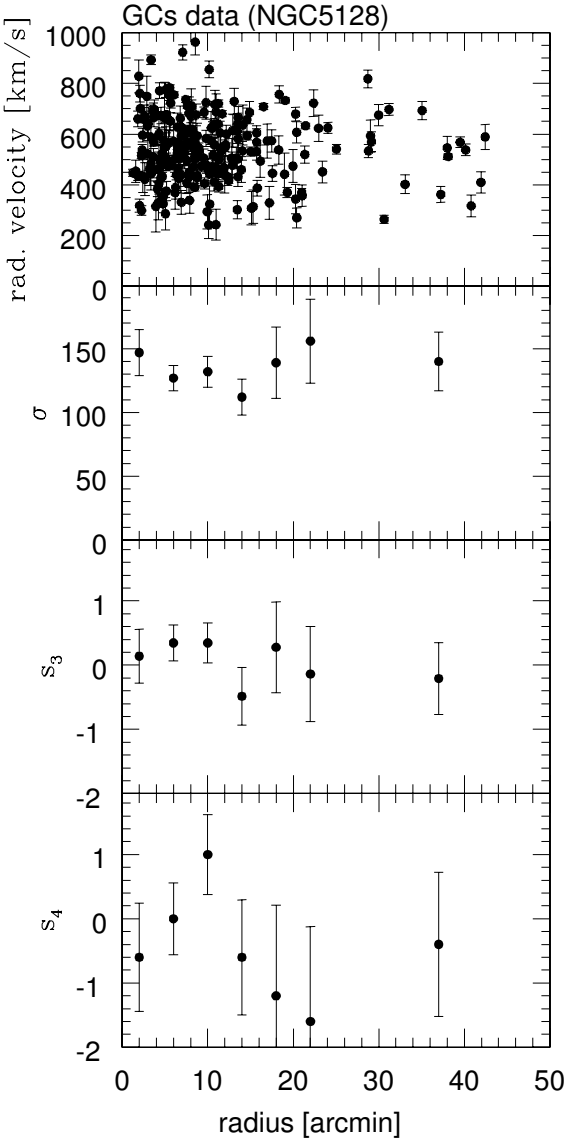

Fig. 1. *Globular clusters kinematics of NGC 5128. From top to bottom: radial velocities of the GCs as function of radius, velocity dispersion as function of radius, asymmetric (s_3) and symmetric departures (s_4) from Gaussian as function of radius.*

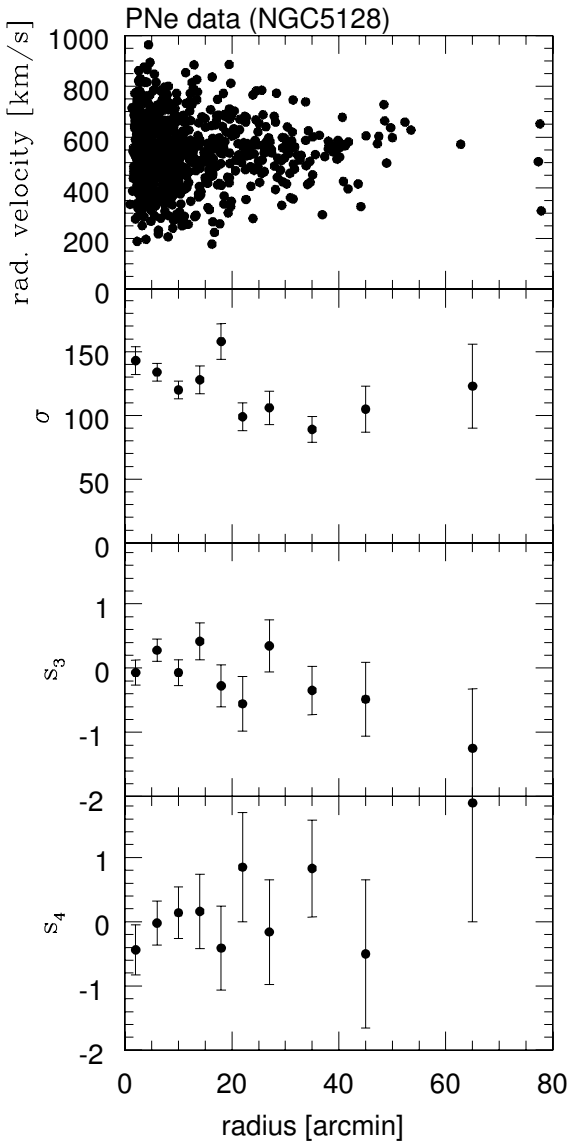

Fig. 2. *Planetary nebulae kinematics of NGC 5128. The meaning of symbols is the same as in Fig. 1. Error bars for the radial velocities are not plotted (see text for details). Note the different scale with respect to Fig. 1.*

and therefore in this paper we have used standard definitions implemented in the NAG routine `G01AAF`. The results which were obtained for GCs and PNe are presented in Table 1 and Table 2, respectively. We calculate velocity dispersion as function of radius and s_3 and s_4 parameters which describe skewness and kurtosis i.e. asymmetric and symmetric departures from the Gaussian (s_3 corresponds to h_3 and s_4 corresponds to h_4 where h_3 and h_4 are quantities extracted from integrated stellar spectra, see van der Marel and Franx 1993).

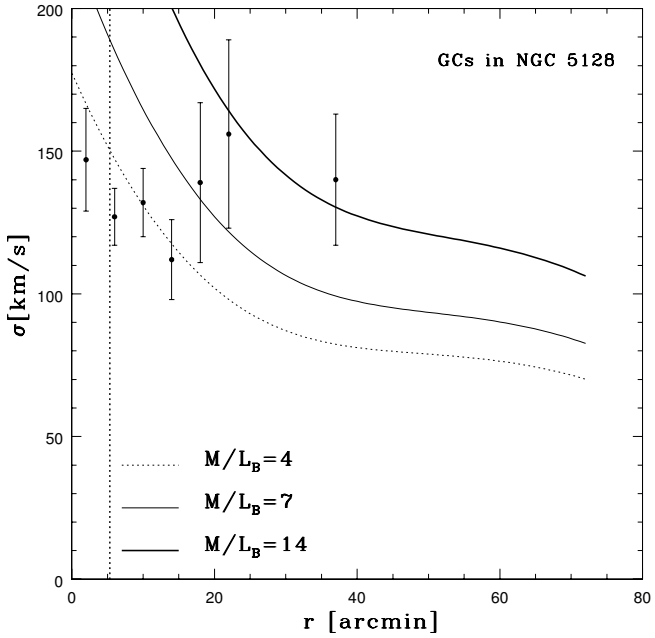

Fig. 3. *Jeans modelling of the globular clusters of NGC 5128. Dotted line is used for the modelling for which $M/L_B = 4$, thin solid line is for $M/L_B = 7$ and thick solid line is for $M/L_B = 14$. Vertical dotted line represents one effective radius. Note that the same scale as in Fig. 4 is used for the sake of comparison.*

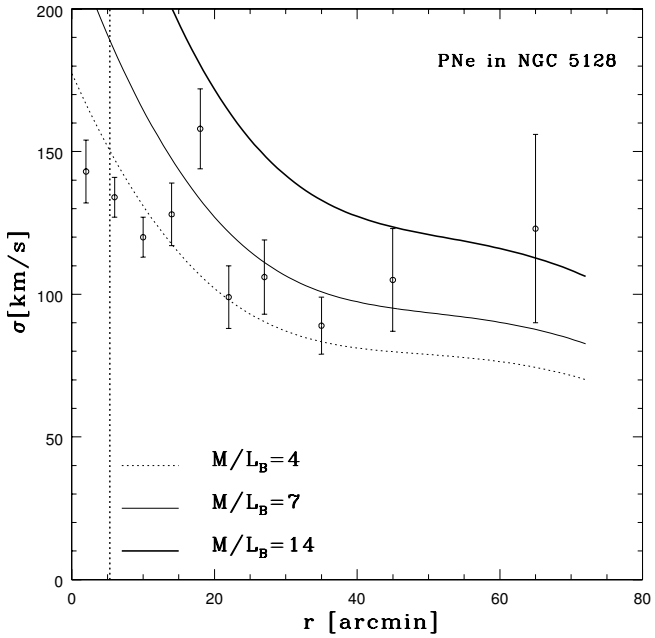

Fig. 4. *Jeans modelling of the planetary nebulae of NGC 5128. Vertical dotted line represents one effective radius. The same modelling was used as in Fig. 3.*

From what one can see from Figs. 1 and 2 the central velocity dispersion of $\sim$ 150 km s^{-1} is not high (see for example the case of the elliptical IC 1459 for which the central velocity dispersion is equal to $\sim$ 350 km s^{-1} in SD05) but it remains fairly constant out to last measured points. The skewness and kurtosis parameters, s_3 and s_4 do not show large departures from the Gaussian and are consistent with zero throughout the galaxy.

We are not trying here to reconstruct the full line of sight velocity distribution, because it is known (see Merritt 1997) that for small samples such as ours which contain less than a few hundred objects per bin this is not possible. We simply calculate s_3 and s_4 parameters and we do not attribute a lot of significance to the numerical values of these parameters, in order to get a hint whether in some bin a significant departure from a Gaussian exists. This is similar to the approach applied by Teodorescu et al. (2005) in their figure 18.

3. X–RAY AND JEANS MODELLING

We briefly present some basic equations, important for the X–ray modelling, which will be applied in the case of NGC 5128. First, it is assumed that spherical symmetry in the galaxy holds, and that the condition of hydrostatic equilibrium is valid:

$$\frac{\mathrm{d}P_{\rm gas}}{\mathrm{d}r} = -\frac{GM(r)\rho_{\rm gas}}{r^2}, \qquad (1)$$

here $M(r)$ is the mass interior to the radius r. Then we assume that the gas obeys the perfect gas law:

$$P_{\rm gas} = \frac{\rho_{\rm gas} k T_{\rm gas}}{\mu m_H}, \qquad (2)$$

where μ = the mean molecular weight for full ionization (taken to be 0.61), and m_H = the mass of the hydrogen atom. From these two equations the total gravitating mass interior to radius r can be calculated as:

$$M(r) = -\frac{kT_{\rm gas} r}{G\mu m_p}\left(\frac{\mathrm{d}\ln\rho_{\rm gas}}{\mathrm{d}\ln r} + \frac{\mathrm{d}\ln T_{\rm gas}}{\mathrm{d}\ln r}\right). \qquad (3)$$

The total mass of the galaxy interior to the radius r is calculated using the following equation taken from Kim and Fabbiano (1995):

$$M_T = 1.8\times10^{12}(3\beta+\alpha)\left(\frac{T}{1\ \mathrm{keV}}\right)\left(\frac{r}{10^{3\prime\prime}}\right) \times\left(\frac{d}{10\ \mathrm{Mpc}}\right) M_\odot, \qquad (4)$$

where the exponent α is related to the temperature ($T \sim r^{-\alpha}$) and in our calculations is taken to be zero, and β is the slope used in the analytic King approximation model and is taken to be $\beta = 0.40$ (Kraft et al. 2003).

The mass-to-light ratio in the B–band is calculated as function of radius r:

$$\frac{M_T}{L_B} = 1.16 \times 10^{-2} 10^{\frac{B}{2.5}} (3\beta + \alpha) \left(\frac{T}{1 \text{ keV}}\right) \times \left(\frac{r}{10^{3\prime\prime}}\right) \left(\frac{d}{10 \text{ Mpc}}\right)^{-1}, \quad (5)$$

where B is the B magnitude of the galaxy inside radius r (Kim and Fabbiano 1995).

Our results obtained using the X–ray methodology are given in Table 3 (mass estimates) and Table 4 (mass-to-light ratio estimates). Error bars given for these estimates take into account the uncertainty for the temperature only. The comparison with the results obtained using GCs and PNe (see Fig. 5) will be given in Section 4.

If we now accept to a first order approximation that the X–ray results discussed above are realistic, we solve the Jeans equation which provides the connection between the anisotropy and the temperature of the hot interstellar gas through which the stars move (Binney and Tremaine 1987):

$$\frac{1}{\ell_*} \frac{\mathrm{d}(\ell_* \sigma_r^2)}{\mathrm{d}r} + \frac{2\beta_* \sigma_r^2}{r} = -\frac{GM(r)}{r^2} + \frac{v_{\rm rot}^2}{r} \quad (6)$$

where σ_r is the radial stellar velocity dispersion, ℓ_* is the stellar luminosity density which corresponds to the radial (σ_r) and transverse (σ_t) stellar velocity dispersions. $v_{\rm rot}$ is the rotation speed (see below) (Hui et al. 1995). A parameter β_* is introduced to describe the nonspherical nature of the stellar velocity dispersion:

$$\beta_* = 1 - \overline{v_\theta^2}/\sigma_r^2, \quad (7)$$

where $\overline{v_\theta^2} = \overline{v_\theta}^2 + \sigma_\theta^2$. For $0 < \beta_* < 1$ the orbits are predominantly radial, in this case the line of sight velocity profile is more strongly peaked than a Gaussian profile (positive s_4 parameter), and for $-\infty \leq \beta_* < 0$ the orbits are mostly tangential, so the profile is more flat–topped than a Gaussian (negative s_4 parameter) (Gerhard 1993). For the stellar luminosity density we adopted the Hernquist (1990) profile:

$$\ell_* = \frac{L}{2\pi} \frac{a}{r} \left(\frac{1}{r+a}\right)^3 \quad (8)$$

where $R_e = 1.8153a$. The projected line–of–sight velocity dispersion is calculated as (e.g. Binney and Mamon 1982, Mathews and Brighenti 2003):

$$\sigma^2(R) = \frac{\int_R^{r_t} \sigma_r^2(r) \left[1 - (R/r)^2 \beta_*\right] \times f_1 \, r\mathrm{d}r}{\int_R^{r_t} f_1 \, r\mathrm{d}r} \quad (9)$$

where

$$f_1 \equiv \ell_*(r)(r^2 - R^2)^{-1/2} \quad (10)$$

and where the truncation radius, r_t, extends to a large distance: in this work it was 50 arcmin (= $9.4R_e$, for GCs) and 80 arcmin (= $15R_e$ for PNe).

The results of this kind of modelling are given in Fig. 3 (for the GCs) and in Fig. 4 (for the PNe). For the sake of comparison both Figures have the same scales. Since both tracers have similar surface density (see below) the same modelling is given in both Figs. 3 and 4. In all the cases the isotropic calculations were performed, i.e. $\beta_* = 0$ was always taken. One can see that a low constant mass-to-light ratio ($M_T/L_B = 4$) can provide a successful fit (interior to ~ 15 arcmin for GCs and interior to ~ 30 arcmin for PNe). An intermediate constant mass-to-light ratio ($M_T/L_B = 7$) can provide a good fit (between ~ 15 and ~ 25 arcmin for GCs and between ~ 30 and ~ 45 arcmin for PNe). A high constant mass-to-light ratio ($M_T/L_B = 14$) provides a good fit in the outer part of the galaxy (beyond ~ 30 arcmin for GCs and beyond ~ 45 arcmin for PNe). This kind of modelling is in agreement with both X-ray estimates and the estimates based on different tracers (see below for details regarding these tracers; see Table 4 for a comparison of the mass-to-light ratios at different radii). The high value of the total mass-to-light ratio implies the existence of dark matter in the outer regions of the galaxy.

4. MASS ESTIMATES OF NGC 5128 BASED ON GCs AND PNe

Evans et al. (2003) introduced a new "tracer mass estimator" which provides an estimate of the enclosed mass from the projected positions and line–of–sight velocities of a given tracer population (such as GCs and PNe). One can assume that the tracer population is spherically symmetric and has a number density which obeys a power law:

$$\rho(r) = \rho_0 \left(\frac{a}{r}\right)^\gamma \quad (11)$$

where a is constant, and radius r ranges between $r_{\rm in}$ and $r_{\rm out}$, inner and outer points of the given population (in this case GCs and PNe), respectively. The parameter γ can be determined using the surface density of the tracer population between $r_{\rm in}$ and $r_{\rm out}$. Evans et al. provide the following formula for the mass enclosed within $r_{\rm in}$ and $r_{\rm out}$ for the isotropic ("iso" in the formulas below) case ("los" stands for line–of–sight):

$$M = \frac{C_{\rm iso}}{GN} \sum_i v_{{\rm los}\,i}^2 R_i, \quad (12)$$

where constant $C_{\rm iso}$ is given as:

$$C_{\rm iso} = \frac{4(\alpha+\gamma)}{\pi} \frac{4-\alpha-\gamma}{3-\gamma} \frac{1-(r_{\rm in}/r_{\rm out})^{3-\gamma}}{1-(r_{\rm in}/r_{\rm out})^{4-\alpha-\gamma}}. \quad (13)$$

The parameter α for an isothermal potential is equal to zero and this value was taken in all the calculations which we performed below. This is a reasonable assumption (see Evans et al. 2003 for details). In this

paper we dealt with the isotropic case, because of the hint of the small departures from the Gaussian distribution (as given by the s_3 and s_4 parameters). The isothermal potential predicts a quasi–constant velocity dispersion profile and this is applicable in the case of NGC 5128 (see Figs. 1 and 2).

As it was argued in Evans et al. (2003) the mass estimator which they derived only calculates the contribution of random motion to the mass. The galaxy NGC 5128 has a large rotational component which is added to the mass calculated using the tracers. Because the rotation curve flattens at ~ 100 km s^{-1} (see Peng et al. 2004b, their Figure 10) this value of the rotation speed $v_{\rm rot}$ was used when the calculation of the rotational component was calculated: $M_{\rm rot}(r) =< v_{\rm rot} >^2 r/G$.

Peng et al. (2004c,b) calculated the value for the γ parameter for both GCs and PNe and these values were used in the present paper: for GCs they found $\gamma = 2.72$ (for *all*, blue and red clusters in the sample, Peng et al. 2004c) and for PNe they found $\gamma = 2.54$. Note that we have used the same value as Peng et al. for the GCs although our sample differs for additional 31 clusters from Woodley et al. (2005). The reason for this is that Peng et al. (2004c) calculated the value for the γ parameter between ~ 6 and ~ 18 arcmin because this region is less affected by incompleteness and the GCs from Woodley et al. sample are found between ~ 17.5 and ~ 20.3 arcmin.

Using the methodology of Evans et al. (2003) and the estimates by Peng et al. (2004b,c) our calculated mass estimates as function of radius are given in Table 3 and our calculated mass-to-light ratio (in solar units in the B-band) are given in Table 4. If one compares the results for the estimates based on GCs and PNe one can see that both tracers predict very similar values of the mass interior to a given radius which may mean that the orbital anisotropies of these two different populations are very similar (noted also in Figs. 1 and 2, especially interior to 20 arcmin where the most of the tracers are present and the estimate of the anisotropies given by the s_3 and s_4 parameters is more acurate). When compared with the results obtained using different techniques found in the literature, the agreement is very good. For example, Kraft et al. (2003) using X–rays found that the total mass interior to 15 arcmin is $M_T = 2 \times 10^{11} M_\odot$ (and $M_T/L_B = 6.64$): this result is represented with the cross symbol in Fig. 5. Peng et al. (2004c) found using GCs that interior to 40 arcmin $M_T = (3.4 \pm 0.8) \times 10^{11} M_\odot$ ($M_T/L_B = 9.7 \pm 2.3$) which is again in agreement with the results found in this paper. Note again, that our two samples differ because we included 31 clusters from Woodley et al. (2005). Finally, Peng et al. (2004b) found for PNe interior to 80 arcmin $M_T = 5 - 6 \times 10^{11} M_\odot$ ($M_T/L_B = 13 - 15$) (open rectangle in Fig. 5). Note that there is a slight difference between Peng et al. and our estimates of the mass interior to 80 arcmin. Although we used the same Evans et al. (2003) technique we did not have error bars for the radial velocity ($\Delta v = 20$ km s^{-1} was taken in all the cases) and this fact produced this minor difference.

We can see in Fig. 5 that dark matter does not dominate interior to ~ 25 arcmin ($\sim 5R_e$) because the total mass-to-light ratio is less that 10. Beyond ~ 25 arcmin the amount of dark matter starts to increase, so at 80 arcmin the mass-to-light ratio of NGC 5128 becomes ~ 14. This is *much* lower than expected: Bahcall et al. (1995) found a relation based on the compilation of the data from the literature that for elliptical galaxies $M_T/L_B = (200 \pm 50) h_0 \times (R/100{\rm kpc})$, which becomes for the adopted $h_0 = 0.70$ at $R = 80$ kpc, $M_T/L_B = 112 \pm 28$.

If we now compare the results for the estimates of the total mass interior to a given radius using both X–rays and the "tracer mass estimator" we can see that interior to ~ 30 arcmin both techniques agree very well. Beyond ~ 30 arcmin the X–rays tend to predict higher inferred mass, so that at 80 kpc the discrepancy between the two becomes significant: X–rays predict $M_X = (11.6 \pm 1.00) \times 10^{11} M_\odot$ whereas the estimate based on the PNe gives $M_T({\rm PNe}) = (5.48 \pm 0.98) \times 10^{11} M_\odot$. A similar discrepancy was noted in the case of the early–type galaxy NGC 1399 (Samurović and Danziger 2006): it was argued that this may be the effect of a contribution of the X–ray gas pressure by the intercluster medium (ICM) (Bertin 2000). However, NGC 5128 does not belong to a cluster and the solution to this problem may be different: the lack of the assumed hydrostatic equilibrium. Very recently, two papers by Humphrey et al. (2006) and Fukazawa et al. (2006) analyzed two samples made using CHANDRA observations (see Section 1 of this paper) assuming hypothesis that hydrostatic equilibrium holds. However, Diehl and Statler (2006) using a sample of 54 normal ellipticals from the CHANDRA archive found that there is no correlation between optical and X–ray ellipticity as would be expected had the gas settled into hydrostatic equilibrium with a given gravitational potential. They found that the hot gas appears to be very disturbed and that the concept of normal ellipticals which host calm, hydrostatic gas needs a revision and argue that X–ray derived radial mass profiles may be in error by a factor of a few. Pellegrini and Ciotti (2006) very recently attempted to reconcile the optical and X–ray mass using the case of the early–type galaxy NGC 3379 (see also SD05) and found that a discrepancy of ~ 2 can be explained by deviations from hydrostatic equilibrium of the hot gas (see also Ciotti and Pellegrini 2004). This may well be the case in the example of NGC 5128 but further detailed analysis is necessary; this paper presents only a first step which quantifies the discrepancy between the X–ray and optical mass.

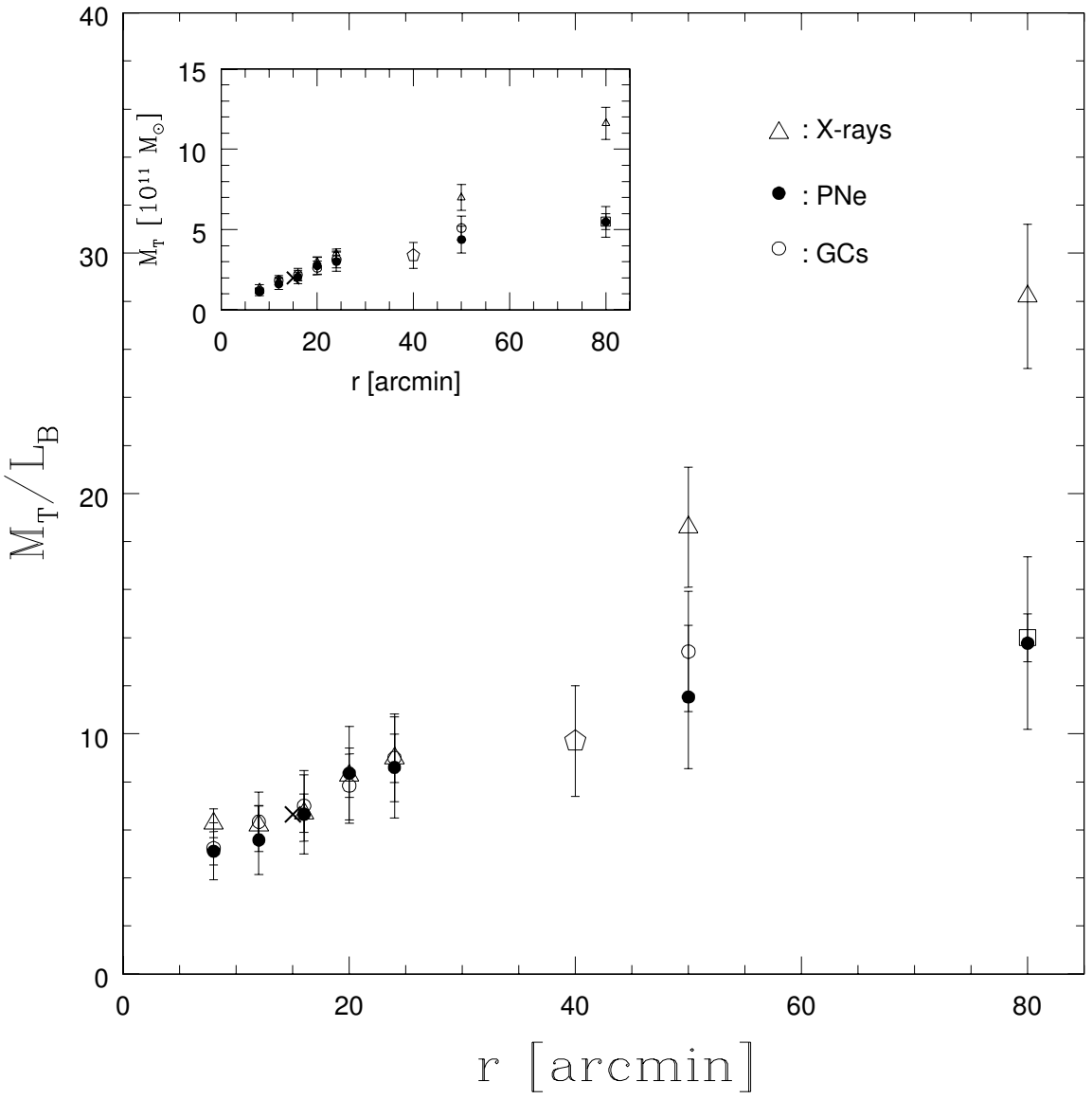

Fig. 5. *Mass and mass-to-light ratio of NGC 5128 using different techniques.* Large box*: mass-to-light ratio in the B–band expressed in solar units as function of radius.* Small inserted box*: Total mass as function of radius expressed in* $10^{11} M_\odot$*. Open triangles are for the estimates based on the X–ray methodology, filled circles are for the results based on the PNe and opened circles are for the data based on the GCs. Point represented with cross is a result based on the X–rays from Kraft et al. (2003), diamond is a result from Peng et al. (2004c) based on the GCs and open rectangle is from Peng et al (2004b) based on the PNe.*

Table 1. Projected velocity dispersion measurements of GCs in NGC 5128.

r (arcmin) (1)	σ (km s^{-1}) (2)	err_σ (km s^{-1}) (3)	s_3 (4)	err_s_3 (5)	s_4 (6)	err_s_4 (7)	N (8)
2	147	18	0.15	0.42	-0.68	0.84	34
6	127	10	0.36	0.28	-0.01	0.56	77
10	132	12	0.32	0.31	0.91	0.62	62
14	112	14	-0.48	0.45	-0.52	0.89	30
18	139	28	0.27	0.71	-1.18	1.41	12
22	156	33	-0.11	0.74	-1.59	1.48	11
37	140	23	-0.21	0.56	-0.47	1.12	19

NOTES – Col. (1): radial bin. Col. (2): velocity dispersion. Col. (3): formal errors for the velocity dispersion. Col. (4): s_3 parameter. Col. (5): formal errors for the s_3 parameter. Col. (6): s_4 parameter. Col. (7): formal errors for the s_4 parameter. Col. (8): number of GCs in a given bin.

Table 2. Projected velocity dispersion measurements of PNe in NGC 5128.

r (arcmin) (1)	σ (km s^{-1}) (2)	err_σ (km s^{-1}) (3)	s_3 (4)	err_s_3 (5)	s_4 (6)	err_s_4 (7)	N (8)
2	143	11	-0.07	0.19	-0.44	0.39	158
6	134	07	0.29	0.17	-0.02	0.34	204
10	120	07	-0.06	0.20	0.14	0.40	147
14	128	11	0.44	0.29	0.16	0.58	72
18	158	14	-0.26	0.33	-0.41	0.65	56
22	99	11	-0.56	0.43	0.85	0.85	33
27	106	13	0.33	0.41	-0.16	0.82	36
35	89	10	-0.31	0.38	0.83	0.76	42
45	105	18	-0.48	0.58	-0.50	1.15	18
65	123	33	-1.25	0.93	1.85	1.85	7

NOTES – Col. (1): radial bin. Col. (2): velocity dispersion. Col. (3): formal errors for the velocity dispersion. Col. (4): s_3 parameter. Col. (5): formal errors for the s_3 parameter. Col. (6): s_4 parameter. Col. (7): formal errors for the s_4 parameter. Col. (8): number of PNe in a given bin.

Table 3. Mass estimates of NGC 5128 using globular clusters, planetary nebulae and X–rays.

r (arcmin) (1)	$M_{\rm GCs}$ ($10^{11}M_\odot$) (2)	err$M_{\rm GCs}$ ($10^{11}M_\odot$) (3)	$M_{\rm PNe}$ ($10^{11}M_\odot$) (4)	err$M_{\rm PNe}$ ($10^{11}M_\odot$) (5)	$M_{\rm rot}$ ($10^{11}M_\odot$) (6)	$M_{\rm X}$ ($10^{11}M_\odot$) (7)	err$M_{\rm X}$ ($10^{11}M_\odot$) (8)
8	0.99	0.14	0.96	0.24	0.18	1.4	0.18
12	1.57	0.30	1.35	0.34	0.27	1.8	0.22
16	1.84	0.38	1.70	0.42	0.36	2.1	0.25
20	2.17	0.43	2.31	0.54	0.45	3.0	0.27
24	2.61	0.52	2.47	0.59	0.54	3.5	0.30
50	3.97	0.74	3.25	0.84	1.13	7.0	0.80
80	—	—	3.68	0.96	1.80	11.6	1.00

NOTES – Col. (1): radius interior to which a given mass is calculated. Col. (2): estimate of the mass based on the GCs expressed in units of $10^{11}M_\odot$. Col. (3): error for the quantity in Col. (2) expressed in the same units. Col. (4): estimate of mass based on the PNe expressed in units of $10^{11}M_\odot$. Col. (5): error for the quantity in Col. (4) expressed in the same units. Col. (6): estimate of the total mass based on the rotation of NGC 5128 expressed in units of $10^{11}M_\odot$. Col. (7): estimate of the total mass based on the X–ray methodology expressed in units of $10^{11}M_\odot$ for $\beta = 0.40$ and $T = 0.29$ keV. Col. (8): error for the quantity in Col. (7) expressed in the same units. The total mass is obtained by summing: $M_{T\,(\rm GCs,PNe)} = M_{\rm GCs,PNe} + M_{\rm rot}$ (see text for details).

Table 4. mass-to-light ratio in the B–band estimates of NGC 5128 using GCs, PNe and X–rays expressed in solar units.

r (arcmin) (1)	$M/L_{\rm GCs}$ $(M_\odot/L^B_\odot)$ (2)	err$M/L_{\rm GCs}$ $(M_\odot/L^B_\odot)$ (3)	$M/L_{\rm PNe}$ $(M_\odot/L^B_\odot)$ (4)	err$M/L_{\rm PNe}$ $(M_\odot/L^B_\odot)$ (5)	$M/L_{\rm X}$ $(M_\odot/L^B_\odot)$ (6)	err$M/L_{\rm X}$ $(M_\odot/L^B_\odot)$ (7)
8	5.24	1.19	5.11	1.19	6.28	0.6
12	6.34	1.44	5.58	1.44	6.20	0.8
16	7.00	1.64	6.65	1.64	6.69	0.8
20	7.84	1.95	8.36	1.95	8.26	0.9
24	9.00	2.10	8.60	2.10	8.98	1.0
50	13.42	2.98	11.53	2.98	18.6	2.5
80	—	—	13.77	3.59	28.2	3.0

NOTES – Col. (1): radius interior to which a given mass-to-light ratio is calculated. Col. (2): estimate of the mass-to-light ratio in the B–band based on the GCs expressed in solar units. Col. (3): error for the quantity in Col. (2) expressed in the same units. Col. (4): estimate of the mass-to-light ratio in the B–band based on the PNe expressed in solar units. Col. (5): error for the quantity in Col. (4) expressed in the same units. Col. (6): estimate of the mass-to-light ratio in the B–band based on the X–rays expressed in solar units. Col. (7): error for the quantity in Col. (6) expressed in the same units.

5. CONCLUSIONS

In this paper we investigated the kinematics calculated from the observations of GCs (Peng et al. (2004a) and Woodley et al. (2005)) and PNe (by Peng et al. 2004b) in the early–type galaxy NGC 5128. From the observational data we calculated velocity dispersions and skewness and kurtosis parameters using standard statistical procedures. We performed an X–ray modelling assuming the hypothesis of hydrostatic equilibrium. Using mass obtained in such a way, we performed the Jeans modelling and compared the modelling results with the observational ones. We also calculated the total mass (and the total mass-to-light ratio) of NGC 5128 using X–ray methodology and a new "tracer mass estimator" in order to compare these estimates.

Our conclusions are as follows.

(1) We show that the departures from the Gaussian (given with the skewness and kurtosis parameters, s_3 and s_4, estimated from the radial velocities) are not large. The similar values of the calculated mass of NGC 5128 at different radii using different tracers suggest that the orbital anisotropies of these two different populations are very similar and small.

(2) We have performed an X–ray modelling of NGC 5128 and solved the Jeans equation. It was found that interior to ~ 25 arcmin ($\sim 5R_e$) the mass is not dominated by dark matter. This is not inconsistent with the previous results (SD05) for 2 early–type galaxies (IC 1459, IC 3370) for which dark matter interior to $\sim 3R_e$ did not appear to dominate. The mass-to-light ratio which we inferred (in the B–band and in solar units) ranges from 4 in the inner regions to 14 in the outer parts of NGC 5128.

(3) Using a new "tracer mass estimator" of Evans et al. (2003) we find that the increase of the total mass of NGC 5128 beyond ~ 25 arcmin ($\sim 5R_e$) implies the existence of dark matter: the total mass rises from $\sim 3\times10^{11}M_\odot$ (corresponds the mass-to-light ratio in the B–band of ~ 9) at $\sim 5R_e$ to $\sim 5.5\times10^{11}M_\odot$ (corresponds the mass-to-light ratio in the B–band of ~ 14). This amount of dark matter (in agreement with Peng et al. 2004c) is lower than expected (see e.g. Bahcall et al. 1995).

(4) We found that, assuming hydrostatic equilibrium, the total mass of NGC 5128 measured at the last observed point, obtained using the X–rays is equal to $11.6\times10^{11}M_\odot$ which is ~ 2 times higher than that found using a "tracer mass estimator". A possible solution to this problem may be the lack of hydrostatic equilibrium in the outer parts of the galaxy, as suggested by Pellegini and Ciotti (2006) and Diehl and Statler (2006).

(5) It remains difficult to draw general conclusions regarding anisotropies in the outer parts of early–type galaxies in general at this point because the sample of galaxies is still too small. Also, in the case of NGC 5128 there are problems regarding small number of observed clusters per galaxy. Judging from the sample of clusters which we used in this paper we did not find large departures from the Gaussian. The similarities of the mass estimates mentioned in the item (1) seem to imply that for NGC 5128 anisotropies are small. SD05 found that for the ellipticals IC 1459 (beyond $\sim 2R_e$) and NGC 3379 (beyond $\sim 1.4R_e$) there is a hint for radial anisotropies. Dekel et al. (2005) recently found, using numerical simulations of disc–galaxy mergers, that for the early–type galaxies the stellar orbits in their outer parts are very elongated. Also, very recently, Teodorescu et al. (2005) found that for PNe in the flattened early–type galaxy NGC 1344 the departures from the Gaussian are small (see their Figure 18).

Acknowledgements – This work was supported by the Ministry of Science and Environmental Protection of the Republic of Serbia through the project no. 14600,

"Structure Kinematics, and Dynamics of the Milky Way". The author gratefully acknowledges the referee, S. Ninković, for his thorough and helpful report.

REFERENCES

Bahcall, N.A., Lubin, L.M. and Dorman, V.: 1995, *Astrophys. J.*, **447**, L81.
Bertin, G.: 2000, Dynamics of galaxies, Cambridge Univ. Press, Cambridge.
Binney, J.J. and Tremaine, S.: 1987, Galactic Dynamics, Princeton Univ. Press, Princeton, NJ.
Binney, J.J. and Merrifield, M.R.: 1998, Galactic Astronomy, Princeton Univ. Press, Princeton, NJ.
Binney, J.J. and Mamon, G.: 1982, *Mon. Not. R. Astron. Soc.*, **200**, 361.
Cappellari et al.: 2006, *Mon. Not. R. Astron. Soc.*, **360**, 1126.
Carollo, C.M., de Zeeuw, P.T., van der Marel, R.P., Danziger, I.J. and Qian, E.E.: 1995, *Astrophys. J*, **441**, L25.
Ciotti, L. and Pellegrini, S.: 2004, *Mon. Not. R. Astron. Soc.*, **350**, 609.
Côté, P., McLaughlin, D.E., Cohen, J.G. and Blakeslee, J.P.: 2003, *Astrophys. J.*, **591**, 850.
De Rijcke, S., Prugniel, P., Simien, F. and Dejonghe, H.: 2006, *Mon. Not. R. Astron. Soc.*, **369**, 1321.
Dekel, A., Stoehr, F., Mamon, G.A., Cox, T.J. and Primack, J.R.: 2005, *Nature*, **437**, 707.
Diehl, S. and Statler, T.S.: 2006, *Astrophys. J.*, submitted, preprint astro-ph/0606215
Dirsch, B., Richtler, T., Geisler, D., Forte, J.C., Bassino, L.P. and Gieren, W.P.: 2003, *Astron. J.*, **125**, 1908.
Dirsch, B., Richtler, T., Geisler, D. et al.: 2004, *Astron. J.*, **127**, 2114.
Evans, N.W., Wilkinson, M.I., Perrett, K.M. and Bridges, T.J.: 2003, *Astrophys. J.*, **583**, 752.
Gerhard, O.: 1993, *Mon. Not. R. Astron. Soc.*, **265**, 213.
Gibson, C.H.: preprint astro-ph/0606073
Fukazawa, Y., Botoya-Nonesa, J.G., Pu, J., Ohto, A. and Kawano, N.: 2006, *Astrophys. J.*, **636**, 698.
Grillmair, C.J., Freeman, K.C., Bicknell, G.V., Carter, D., Couch, W. J., Sommer–Larsen, J. and Taylor, K.: 1994, *Astrophys. J.*, **422**, L9.
Hernquist, L.: 1990, *Astrophys. J.*, **356**, 359.
Humphrey, P.J., Buote, D.A., Gastaldello, F., Zappacosta, L., Bullock, J.S., Brighenti, F. and Mathews, W.G.: 2006, *Astrophys. J.*, **646**, 899.
Hui, X., Ford, H.C., Ciardullo, R. and Jacoby, G.H.: 1993, *Astrophys. J.*, **414**, 463.
Hui, X., Ford, H.C., Freeman, K.C. and Dopita, M.A.: 1995, *Astrophys. J.*, **449**, 592.
Israel, F.P.: 1998, *Astron. Astrophys. Rev.*, **8**, 237.
Kim, D.–W. and Fabbiano, G.: 1995, *Astrophys. J.*, **441**, 182.
Koopmans, L.V.E. and Treu, T.: 2003, *Astrophys. J.*, **583**, 606.
Kraft, R.P., Vázquez, S.E., Forman, W.R., Jones, C., Murray, S.S., Hardcastle, M.J., Worrall, D.M. and Churazov, E.: 2003, *Astrophys. J.*, **592**, 129.
Kleinheinrich, M., Schneider, P., Erben T., Schirmer, M., Rix, H.–W., Meisenheimer, K. and Wolf, C.: 2003, preprint astro-ph/0304208
Kronawitter, A., Saglia, R.P., Gerhard, O. and Bender, R.: 2000, *Astron. Astrophys. Suppl. Series*, **144**, 53.
Mamon, G.A. and Łokas, E.L.: 2005, *Mon. Not. R. Astron. Soc.*, **362**, 95.
Mathews, W.G. and Brighenti, F.: 2003, *Ann. Rev. Astron. Astrophys.*, **41**, 191.
Merritt, D.: 1997, *Astron. J.*, **114**, 228.
Mould, J.R., Oke, J.B., de Zeeuw, P.T. and Nemec, J.M.: 1990, *Astron. J.* 99, 1823.
Pellegrini, S. and Ciotti, L.: 2006, *Mon. Not. R. Astron. Soc.*, **370**, 1797.
Peng, E.W., Ford, H.C. and Freeman, K.C.: 2004a, *Astrophys. J. Supp. Series*, **150**, 367.
Peng, E.W., Ford, H.C. and Freeman, K.C.: 2004b, *Astrophys. J.*, **602**, 685.
Peng, E.W., Ford, H.C. and Freeman, K.C.: 2004c, *Astrophys. J.*, **602**, 705.
Pierce, M., Beasley, M.A., Forbes, D.A., Bridges, T., Gebhardt, K., Faifer, F.R., Forte, J.C., Zepf, S.E., Sharples, R., Hanes, D.A. and Proctor, R.: 2006, *Mon. Not. R. Astron. Soc.*, **366**, 1253.
Prada, F., Vitvitska, M., Klypin, A., Holtzman, J.A., Schlegel, D.J., Grebel, E.K., Rix, H.-W., Brinkmann, J., McKay, T.A. and Csabai, I.: 2003, *Astrophys. J.*, **598**, 260.
Rejkuba, M.: 2004, *Astron. Astrophys.*, **413**, 903.
Richtler, T., Dirsch, B., Gebhardt, K. et al.: 2004, *Astron. J.*, **127**, 2094.
Romanowsky, A.J., Douglas, N.G., Arnaboldi, M., Kuijken, K., Merrifield, M.R., Napolitano, N.R., Capaccioli, M. and Freeman, K.C.: 2003, *Science*, **5640**, 1696.
Samurović, S. and Danziger, I.J.: 2005, *Mon. Not. R. Astron. Soc.*, **363**, 769 (SD05).
Samurović, S. and Danziger, I.J.: 2006, *Astron. Astrophys.*, **458**, 79.
Sivakoff, G.R., Sarazin, C.L. and Carlin, J.L.: 2004, *Astrophys. J.*, **617**, 262.
Sluis, A.P.N. and Williams, T.B.: 2006, *Astron. J.*, **131**, 2089.
Statler, T.S., Smecker–Hane, T. and Cecil, G.N.: 1996, *Astron. J.*, **111**, 1512.
Teodorescu, A.M., Méndez, R.H., Saglia, R.P. et al.: 2005, *Astrophys. J.*, **635**, 290.
Thomas, J., Saglia, R.P., Bender, R., Thomas, D., Gebhardt, K., Magorrian, J., Corsini, E.M. and Wegner, G.: 2005, *Mon. Not. R. Astron. Soc.*, **360**, 1355.
Tonry, J.L.: 1983, *Astrophys. J.*, **266**, 58.
Treu, T., Koopmans, L.V.E., Sand, D.J., Smith, G.P. and Ellis, R.S: 2003, in the proceedings of IAU Symposium 220 "Dark matter in galaxies", S. Ryder, D.J. Pisano, M. Walker, and K. Freeman (eds.), 159.
Treu, T. and Koopmans, L.V.E.: 2002, *Astrophys. J.*, **575**, 87.
van der Marel, R.P. and Franx, M.: 1993, *Astrophys. J.*, **407**, 525.
van der Marel, R.P.: 1991, *Mon. Not. R. Astron. Soc.*, **253**, 710.
Woodley, K.A., Harris, W.E. and Harris, G.L.H.: 2005, *Astron. J.*,**129**, 2654.

NOTES ADDED IN PROOF:

In the course of preparing this manuscript, preprint of the accepted paper by Woodley (2006) appeared, in which a much higher mass was claimed based on the new (but still unpublished) sample of GCs of NGC 5128. For example, Woodley finds within $\sim$ 15 kpc the total mass of $4 \times 10^{11} M_{\odot}$. In this paper, as well as in the aforementioned Peng et al. papers, the total mass within $\sim$ 15 kpc is $\sim 2 \times 10^{11} M_{\odot}$. The reason for this discrepancy lies in the parameter γ (Woodley, private communication): in this paper $\gamma_{\rm GC} = 2.72$ was used and Woodley used $\gamma_{\rm GC} = 3.65$. Woodley (private communication) claims that Peng et al. (2004b,c) erroneously used surface density slope instead of the volume density slope. Note, however, that using completely different technique, such as the X–ray methodology (Kraft et al. 2003), half of this higher mass is obtained: $\sim 2 \times 10^{11} M_{\odot}$ within $\sim$ 15 kpc. At $\sim$ 50 kpc Woodley (2006) finds the total mass equal to $1.3 \pm 0.5 \times 10^{12} M_{\odot}$ which is again not consistent with the estimate based on X–rays, yielding $7.0 \pm 0.8 \times 10^{11} M_{\odot}$. As one can see from Fig. 5, the X-ray mass is in very good agreement with that obtained using TME inside $\sim$ 50 kpc. This shows that the variations in the parameter γ may cause huge discrepancies. It is worth noting that both Peng et al. (2004b,c) and Woodley (2006) calculated the parameter γ outside of 5 kpc because of the incompletness; this may have influenced the true value of the parameter γ. That is why we decided to calculate the total mass of this galaxy using another estimator which uses point tracers (such as GCs and PNe) but *does not* depend on the density slope. Bahcall and Tremaine (1979) give the following formula (which uses the same notation as previously in this paper) for the isotropic case:

$$M = \frac{16}{GN} \sum_i v_{{\rm los}\,i}^2 R_i.$$

Using this formula we found, for example, that inside $\sim$ 16 kpc the total mass obtained in this way using GCs, is equal to $\sim 1.8 \times 10^{11} M_{\odot}$ which is very close to the value obtained using the Evans et al. TME ($M_{\rm GCs} = 1.84 \times 10^{11} M_{\odot}$, see Table 3). Within $\sim$ 50 kpc, using the formula from Bahcall and Tremaine (1979) and the sample of GCs, the mass becomes equal to $\sim 3.3 \times 10^{11} M_{\odot}$, again very close to the estimate based on the Evans et al. TME ($M_{\rm GCs} = 3.97 \times 10^{11} M_{\odot}$, see Table 3). These two estimates, at two different radii, are based only on the *random* motions while the rotational part was not taken into account. Therefore, for the estimate of the total mass the appropriate values from the Column 6 found in the Table 3 must be added. It is also important to inspect Figs. 3 and 4 in which the Jeans modeling was presented: it is obvious that much higher masses cannot provide a satisfactory fit to the observed velocity dispersion (the Jeans modelling is not present in Woodley 2006). The mass-to-light ratio in the B–band between $\sim$ 4 and $\sim$ 14 provides a good fit to the mass-to-light ratio for both GCs and PNe. The mass-to-light ratio in the B-band inferred by Woodley (2006), equal to 52 (interior to 50 kpc), seems to be too high.

As a final attempt to calculate the total mass of NGC 5128 we decided to use the formula which comes from the paper by Bertin et al. (2002) and is valid for a stationary stellar system for which the scalar virial theorem can be written as:

$$\frac{G \Upsilon L_*}{R_e} = K_V \sigma_0^2,$$

where Υ is the *stellar* mass-to-light ratio in the given band, R_e is the effective radius and σ_0 is the central velocity dispersion referred to an aperture radius of $R_e/8$. K_V is the so-called "virial coefficient" which takes into account the projection effects. It was shown recently by Cappellari et al. (2006) that $K_V = 5 \pm 0.1$ for a sample of early-type galaxies at redshift $z \sim 0$. From this equation the total dynamical mass is:

$$M_{\rm dyn} = K_V \frac{\sigma_0^2 R_e}{G}.$$

Inserting the aforementioned value for $K_V = 5$, $\sigma_0 =$ 150 km/s, and $R_e = 5.3$ kpc one obtains the total dynamical mass of NGC 5128: $M_{\rm dyn} = 1.34 \times 10^{11} M_{\odot}$. This value takes into account only *random* motions and it does not take into account the rotational support so it is necessarily lower than the true value. Taking into account M_{rot} from Table 3 one gets the total mass of $\sim 3 \times 10^{11} M_{\odot}$ which is lower (but not much) than the value obtained using GCs and PNe, but is *much* lower than the value inferred by Woodley (2006).

To summarize, one can conclude that the results for the total mass (and the mass-to-light ratio) of NGC 5128 obtained in this paper are roughly correct, because the results obtained using various techniques are consistent (except for the last measured point, but this may be due to some real physical effect as said in the item 4 above). Also, the results of the Jeans modelling provide an important additional evidence to the roughness of the results presented in this paper.

It is certain that the galaxy NGC 5128 will be studied in more detail in the years to come, and the question of its total mass will be addressed using more sophisticated observations and models removing the discrepancies found in the literature present at this stage.

REFERENCES

Bertin, G., Ciotti, L. and Del Principe, L.: 2002, *Astron. Astrophys.*, **386**, 149.

Cappellari, M., Bacon, R., Bureau, M., Damen, M.C., Davies, R.L., de Zeeuw, P.T., Emsellem, E., Falcón-Barroso, J., Krajnović, D., Kuntschner, H., McDermid, R.M., Peletier, R.F., Sarzi, M., van den Bosch, R.C.E. and van de Ven, G.: 2006, *Mon. Not. R. Astron. Soc.*, **366**, 1126.

Woodley, K.A.: 2006, *Astron. J.*, accepted, preprint astro-ph/0608497

КИНЕМАТИКА ГЛОБУЛАРНИХ ЈАТА И ПЛАНЕТАРНИХ МАГЛИНА И ЕМИСИЈА У Х– ПОДРУЧЈУ У ЕЛИПТИЧНОЈ ГАЛАКСИЈИ NGC 5128

S. Samurović

Astronomical Observatory, Volgina 7, 11160 Belgrade 74, Serbia

UDK 524.7–42–73
Оригинални научни рад

У раду су дате процене масе галаксије NGC 5128 засноване на различитим индикаторима (tracers) масе, глобуларним јатима и планетарним маглинама. Ове процене су упоређене са проценом заснованом на методологији X- зрака и утврђено је да се сва три приступа врло добро слажу до удаљености од 25 лучних минута; на удаљеностима већим од 25 лучних минута маса заснована на X- зрацима је превелика у односу на ону засновану на глобуларним јатима и планетарним маглинама. Дискутована су нека могућа решења овог проблема. У раду је такође решена Џинсова (Jeans) једначина и предвиђања за дисперзију брзина која следе из ње су упоређена са посматраним вредностима, које се простиру до ~ 8 ефективних радијуса у случају глобуларних јата и ~ 15 ефективних радијуса у случају планетарних маглина. Пронађено је да унутар ~ 25 лучних минута (~ 5 ефективних радијуса) тамна материја не доминира зато што је однос маса–сјај у B–појасу у сунчевим јединицама мањи од 10. Процена укупног односа маса–сјај заснована на глобуларним јатима и планетарним маглинама расте до ~ 14 (на ~ 80 лучних минута) што говори у прилог постојању тамне материје у спољним областима галаксије NGC 5128.